P1.19 Rainfall estimation over the Taiwan Island from TRMM/TMI data

Wann-Jin Chen[1], Ming-Da Tsai[1], Gin-Rong Liu[2], Jen-Chi Hu[1] and Mau-Hsing Chang[1]

[1]Dept. of Applied Physics, Chung Cheng Institute of Technology, National Defense University

[2]Center for Space and Remote Sensing Research, National Central University

I. Introduction

The Taiwan is a mountainous island, recent overdevelopment of hill slope has made the water and soil conservation more difficult. In the advent of storm's heavy rainfall, mudslide is likely to strike the upstream mountainous regions, leading to serious mud accumulation or flood in rivers and reservoirs or even water and soil loss against national economy and national security. Therefore, it is the focus for the meteorology community to improve weather forecasting technology for storm's heavy rainfall and minimize or prevent the loss from catastrophic rainfall in an efficient way.

With rapid development of satellite technology in recent years, satellite microwave data has become a major tool for rainfall research on an international basis. This is because meteorological satellite is a simplest method to monitor and track effectively all catastrophic rainfall systems from surrounding sea areas. And, this helps to understand the process and strength of rainfall systems, thereby providing all information required for flood prevention. This laboratory once applied satellite microwave image data to study rainfall over the ocean and obtain good results (Chen and Li, 2000; Chen and Li, 2002; Hu, 2002; Chen, 2004). To have a further observation and deeper understanding of rainfall system's development over Taiwan land, microwave image data shall be applied to study the features and retrieval of land rainfall. Now, it is the first time that Scattering - Index Method is applied to research of rainfall over Taiwan land. It is expected to set up a mechanism for monitoring and tracking catastrophic rainfall system.

This paper aimed to study rainfall retrieval over Taiwan land using Scattering - Index Method developed by Grody (1991), with the entire flow process shown in Fig. 1. The steps include: data collection and processing, land rainfall retrieval and verification of retrieval results. Firstly, the cases of TRMM/TMI (Tropical Rainfall Measuring Mission/TRMM Microwave Imager) passing through Taiwan land and the corresponding data of land rainfall observation stations (ARMTS, rain gauge data of Automatic Rainfall and Meteorological Telemetry System measurements of Taiwan) were collected and interpolated into the grid points in the region of Taiwan. Infrared (IR) satellite cloud figures were used to determine cloud-free cases in Taiwan (representing non-scattering atmospheric structure), while the data in this time interval were applied for analysis of surface characteristics. By substituting the data into Scattering - Index Method (SI) developed by Grody (1991), the equation was shown in Eq (1). Through simulation of high-frequency Tb85V by low-frequency Tb19V and Tb22V channels, coefficients A1, A2, A3 and A4 could be obtained from SI equation via linear regression, thereby setting up a scattering index equation (SIL) of Taiwan land.

$$\mathrm{SIL} = [\,A_1 + A_2(\mathrm{Tb19V}) + A_3(\mathrm{Tb22V}) + A_4(\mathrm{Tb22V})^2\,] - \mathrm{Tb85V} \qquad (1)$$

Secondly, SIL was matched to RR, such that SIL's rainfall threshold could be defined and rainfall retrieval equation of Taiwan land be set up. According to the research findings of Ferraro and Marks (1995), the relationship between SIL and RR was:

$$\mathrm{RR} = a\,\mathrm{SIL}^{\,b} \qquad (2)$$

There are coefficients a, b for RR of Taiwan land. Finally, the retrieval results of rainfall estimates were demonstrated and discussed based on the truth value of land rainfall observation stations.

II. Data Collection and Processing

Region of research: 21.5~25.5^{o}N; 120~122$^{o.}$E, covering Taiwan and nearby sea areas. During the 2004 Typhoon Mindulle and Typhoon Aere, we collected data including TRMM satellite observed data incorporating TMI, VIRS (Visible Infrared Scanner) and the rainfall data from ARMTS over the Taiwan land. Meanwhile, it identified non-scattering atmospheric conditions using GOES-9 satellite data. So, data collection includes two elements: 1, satellite data, 2, observed data from land observation stations. Next, the collected satellite data and ground-based observed data are interpolated into the grid points in the region of interest, which allow for identification of terrain and contribute to research of land rainfall with TMI microwave image data.

(I) Data Collection

1, Satellite Data

(1) TRMM/TMI, VIRS

Since its launch on 27, Nov, 1997 jointly by the U.S. and Japan, TRMM satellite started to observe rainfall in tropic zones between 40°N and 40°S. The observed data can be applied to study abnormal climate changes (e.g. El Nino), and improve physical rainfall mechanism of global environmental transition mode as well as the process of dynamic and thermal change of tropic zone rainfall system. With a track height of 350 km before August, 2001, it moved around the earth at 35°inclination and with a period of about 92 minute for an expected three-year observation. To prolong its service life, the height of satellite was raised to 402 km after August, 2001. Onboard TMI is a passive microwave radiometer, one of useful tools for observing rainfall in tropic zones. Other observation apparatuses include first-ever onboard active Precipitation Radar (PR), visible light and infrared detector, Clouds and the Earth Radiant Energy System (CERES) and Lightning Imaging Sensor (LIS). Fig. 2 depicts the scanning mode and resolutions of different sensors on board TRMM satellite (Kummerow et al., 1998).

With observed data of TRMM satellite, the case study focused on Typhoon Mindulle and Typhoon Aere from June to August, 2004. It also conducted land rainfall retrieval research based on brightness temperature of TMI microwave channel and 10.8 μm infrared brightness temperature of VIRS. TMI data, a kind of Level - 1B11 data, is represented by microwave brightness temperature of 10 km resolution after radiation calibration and geographic registration. The data in this paper include brightness temperature of Tb19V, Tb21V and Tb85V microwave channels. In terms of VIRS data, this paper applied VIRS Level - 1B01 $IRTb_{11}$ radiation data, with a resolution of 2.2 km (Kummerow et al., 1998). With a range of 720 km, it presents advantages of rainfall observation in parallel with TMI, and provides a reference basis for testing TMI satellite data.

(2) GOES-9 Satellite Data

GOES-9 satellite is located at equator of 155°E, about 35,800km away from the earth. It stands still in relative to the earth while moving synchronously with the autorotation of earth. GOES-9 moved over western Pacific Ocean in lieu of GMS-5 since 22, May, 2003, and provided satellite images for local regions. Thus, it is possible to monitor clearly the cloud layer and cloud cluster over western Pacific Ocean around the clock (website of Central Weather Bureau). In this paper, GOES-9 infrared (11 μm) cloud map from Satellite Center of CWB is used to judge cloud-free time interval prior to the advent of typhoon, thus serving the case study of non-scattering state under some atmospheric conditions.

2, Land Rainfall Data

Rain Rate (RR) is sourced from the rainfall data of Taiwan's automatic rainfall observation stations, as listed in DBAR (Data Bank for Atmosphere Research) of Atmospheric Department of Taiwan University. As such, this paper intends to study and analyze the data of 362 rain gauge across Taiwan, shows in Fig. 3, in collaboration with time of passage of 2004 Typhoon Mindulle and Typhoon Aere through Taiwan land.

(II) Data Processing

This paper focused on land rainfall in Taiwan, with a scope of research: 21.5° ~ 25.5° N; 120° ~ 122° E. The reference data of different resolutions include: satellite data, observed data of automatic observation stations and altitude, which are interpolated into a grid coordinate of 0.1° * 0.1° of Taiwan for future data processing. It covers Taiwan and nearby sea areas.

In this research region, there are 861 grid points of 0.1° * 0.1°, whereby the earth surface are categorized into: 217 points over land (white), 157 points along coast (black) and 487 points over sea (grey), as shown in Fig. 4. After classification of property, the radiance over land is free from the interference of that over sea. In this paper, 217 points over land (white) are applied for research of land rainfall retrieval.

III. Rainfall Retrieval Algorithms

(I) Equation of Scattering Index over Land (SIL)

Located at a subtropical region, Taiwan is a mountainous island, with the mountains accounting for 3/5 of its total area, and Central Mountain extending from north to south. Owing to its unique terrain and atmospheric conditions, together with TRMM/TMI satellite data, the observing frequency and resolution of satellite data differ from SSM/I previously applied by Grody (1991) and Ferraro (1995). This paper aimed to build up scattering index equation of SIL using CH3, CH5 and CH8 (Tb19V, Tb21V and Tb85V) in TRMM/TMI microwave channels. According to the theory of Grody (1991), the energy received from satellite microwave sensor is sourced from the earth surface under non-scattering atmospheric conditions. Simulating Tb85V by Tb19V and Tb21V in TRMM/TMI microwave channels, the relationship is shown below:

$$Tb85V = A_1 + A_2(Tb19V) + A_3(Tb21V) + A_4(Tb21V)^2 \quad (3)$$

An equation of scattering index was set up using TRMM/TMI microwave image data. Firstly, collect cloud-free cases as non-scattering cases prior to invasion of typhoon. This paper has collected the cases of TRMM satellite passing through Taiwan, prior to invasion of Typhoon Mindulle and Typhoon Aere. And, GOES-9 infrared cloud figures are used to identify the duration of cloud-free state, which may serve as the cases of non-scattering atmospheric conditions in Taiwan. As Tb85V is simulated by Tb19V and Tb21V data in TRMM/TMI microwave image data, the relationship can be obtained from above Eq. (3) through linear regression:

$$Tb85V = 220.878 - 0.747(Tb19V) + 0.554(Tb21V) + 0.00147(Tb21V)^2 \quad (4)$$

Based on brightness temperature of Tb85V, the Root Mean Square Error is 1.84 K, and correlation coefficient is 0.76, with the relationship of brightness temperature shown in Fig.5. The equation of scattering index for Taiwan land may be obtained from above equations using TRMM/TMI microwave image data:

$$SIL=[220.878-0.747(Tb19V)+0.554(Tb21V)+0.00147(Tb21V)^2]-Tb85V \quad (5)$$

(II) Retrieval Equation of Rainfall over Taiwan Land

Firstly, rainfall threshold of SIL in Taiwan was defined. Secondly, retrieval of land rainfall equation was affected with observed data of rain gauge and SIL value.

1, Rainfall Threshold of SIL over Taiwan Land

Based on collected microwave image data of TRMM/TMI during invasion of Typhoon Mindulle and Typhoon Aere, SIL could be obtained according to above-specified scattering index equation, Eq.(5), and then matched to the observed rainfall data from rain gauge. The statistics showed that, there are 1659 points of 0 mm/hr rainfall, with the distribution shown in Fig.6. Mean value of SIL is 0.83 K, and standard deviation 3.51 K. According to the statistical analysis, two-times standard deviation serves as a confidence interval for sampling purpose (95 % confidence level).

The aforementioned statistical analysis showed that, SIL is -6.19 K < SIL < 7.85 K in case where land rainfall is 0 mm/hr. Therefore, rainfall threshold of SIL over Taiwan land was defined as 8 K. As illustrated in Fig. 7, there are extremely big SIL up to 40 K, since satellite passes through Taiwan within 1m. This leads to time difference owing to nearly instantaneous rainfall observed from TMI microwave image data and integral land rainfall data. In addition, TMI microwave image data represent observed data of a certain area, with its Field of View (FOV) resolution as 10 km, while the observed data from rain gauge is just sampling data of some points, so both of them differ from each other with respect to space resolution.

2, Rainfall Retrieval over Taiwan Land

The rainfall retrieval equation over Taiwan land depends upon satellite data and land rainfall observation data in the event of invasion of Typhoon Mindulle. There are five cases from June 30 to July 2. Fig.7 depicts the relationship between SIL from TRMM/TMI satellite data and land rainfall observed from ARMTS. The relational expression is shown in Eq. (2) (Ferraro and Marks, 1995). The retrieval formula of rainfall over Taiwan land could be obtained from statistical regression algorithm:

$$RR\ (mm/hr) = 0.126\ SIL^{1.239} \quad (6)$$

Secondly, the rainfall equation is assessed in this paper, and rainfall threshold of SIL (8 K) was substituted into Equ. (6) to find the corresponding RR, a value of 1.6 (mm/hr). So, the land rainfall retrieval equation is suitable for rainfall system over 1.6 mm/hr. Similarly, the land rainfall retrieval algorithm developed by Ferraro and Marks (1995) and the researcher was used to estimate and compare the rainfall over

Taiwan land, thus providing a further insight into this retrieval formula.

IV. Results and Discussions

(I) Verification of Estimated Land Rainfall

With microwave image data of TRMM/TMI, the land rainfall retrieval algorithm developed by Ferraro and Marks (1995) and the researcher is used to estimate and compare the rainfall over Taiwan land, thus providing a further insight into this retrieval formula. In short, the result derived from retrieval methods by Ferraro and Marks (1995), as Eqs. (7), (8) and the research is represented by LRCT (Land Rainfall Retrieval by Chen and Tsai) and LRFM (Land Rainfall Retrieval by Ferraro and Marks).

$$SIL_{LRFM} = 451.9–0.44(Tb19V)–1.775(Tb22V) + 0.00575(Tb22V)^2 - Tb85V \quad (7)$$

$$RR_{LRFM}\ (mm/hr) = 0.00513\ (SIL^{1.9468}) \quad (8)$$

Firstly, 74 effective sample points (non-beam-filling) are selected during the outbreak of Typhoon Mindulle, and point-to-point comparison is performed by taking the land observation points as truth value, with the results listed in Table 1. On a comparable basis, the mean rainfall estimated by LRCT is similar to observed value over land, a difference of 0.01 mm/hr, whereas the estimated value of LRFM has a margin of 5.81 mm/hr to the observed value. For the Root Mean Square (RMS) between them, RR estimated by LRCT is very close to observed value over land, a difference of 5.14 mm/hr, whereas the estimated value of LRFM has a margin of 7.13 mm/hr to the observed value. The mean rainfall and RMS show that, the rainfall derived from land rainfall equation of LRFM is obviously underestimated.

Secondly, there are two reference examples of TRMM/TMI during invasion of Typhoon Aere (serial number of track: # 38609, # 38613), whereby effective samples are selected using infrared satellite images of VIRS. All together, 23 data points are taken as samples for testing the estimated value of land rainfall.

The statistical results are listed in Table 2, wherein the mean rainfall from land observation data is 5.53 mm/hr, and that from LRCT is 6.1 mm/hr, with the Root Mean Square Error as 3.48 mm/hr. Conversely, the mean rainfall estimated from rainfall retrieval equation of Ferraro is 2.71 mm/hr, with the Root Mean Square Error up to 4.28 mm/hr. So, LRCT has a better performance than LRFM for verification of land rainfall estimates during invasion of Typhoon Aere. Furthermore, the land rainfall estimated by LRFM is obviously underestimated in Taiwan land during these verifications.

To further explore the quantified land rainfall, the land rainfall data of all effective samples are compared with satellite-estimated rainfall, as shown in Fig. 8. There are 97 samples points for verification of estimated quantity of entire land rainfall. The rainfall estimated by LRFM is obviously underestimated (about 38%) as compared to the observed rainfall over land. However, the rainfall estimated by LRCT is very close to the observed value over Taiwan land (1%).

(II) Influence of Terrain upon Satellite- Estimat -ed Land Rainfall

This session, according to Typhoon Mindulle in different time sequences, this paper strives to explore the difference of land rainfall from satellite data, which may vary under the influence of different wind farms and terrains. Fig. 9 is a track chart of Typhoon Mindulle provided by Central Weather Bureau, whereby this typhoon moved from southeast to northeast. Taiwan land is greatly covered and influenced by this typhoon during 1 ~ 2 of July.

Therefore, LRCT drafted a rainfall difference distribution map of TRMM/TMI satellite-estimated land rainfall and land-based rainfall data observed during 1 ~ 2 of July, together with the data of ground surface weather map of the time. Four time points are available: 2004 / 07 / 01 04:52 UTC (#37769) , 2004 / 07 / 01 11:24 UTC (#37773), 2004 / 07 / 02 05:35 UTC (#37785), 2004 / 07 / 02 12:07 UTC (#37789), as shown in Figs. 10 ~ 13. On July 1, this typhoon was located at southeastern sea of Taiwan, and eastern side of Central Mountain was windward side, and western side was leeward side for the wind direction. So, as seen in the rainfall difference distribution map (Figs. 10, 11), satellite-estimated rainfall at eastern side (windward side) is obviously underestimated, and that at western side overestimated.

This typhoon gradually moved northwards, arrived at Taipei region on July 2, and went to sea from TAMSUI River Estuary. As seen in the land weather map, the western side of Central Mountain was windward side and eastern side was leeward side for the wind direction of that time. As such, the rainfall in overall rainfall distribution map (Figs. 12, 13) differed a little from that on July 1. In other words, satellite-estimated rainfall at western side (windward side) was obviously underestimated, and that at eastern side overestimated. Based on the estimated land rainfall during invasion of Typhoon Mindulle, in addition to consideration of radiation reflected by the strength of rainfall system, the influential factors, such as terrain and wind farms, shall also be considered so as to improve the accuracy of land rainfall estimates.

V. Conclusions

With the help of Scattering - Index Method, this paper conducted rainfall retrieval over Taiwan land using TRMM/TMI satellite microwave image data. In terms of land rainfall retrieval, GOES-9 infrared satellite cloud figure is firstly used to identify cloud-free conditions, which may serve as non-scattering atmospheric conditions to set up a scattering index equation of Taiwan land, as shown in Eq. (5). Secondly, through statistical analysis of 0 mm/hr rainfall, it is possible to identify the rainfall threshold of Scattering - Index Method as 8K. By deducting the threshold of 8 K, and performing data regression for other land rainfall, the land rainfall equation of Taiwan is shown in Eq. (6).

In terms of verification of land rainfall estimates, quantified rainfall retrieval is verified according to land rainfall cases during Typhoon Mindulle and Typhoon Aere. By comparing LRCT and LRFM in this verification, LRCT is more suitable to the rainfall over Taiwan land, and total estimated rainfall conforms to the observed value from land observation stations. The mean rainfall estimated by LRCT is 14.14, 6.10 mm/hr, with the Root Mean Square Error as 5.14 and 3.48 mm/hr. SIL becomes stronger with the increasing strength of rainfall system. The observed rainfall from rain gauge shows a different distribution with changing terrains and wind directions, in addition to its correlation with the strength of rainfall system. The research findings indicate that satellite-estimated rainfall is obviously underestimated at windward side, and overestimated at leeward side.

This paper made efforts to study the land rainfall with a single formula. In the future, it is scheduled to perform the study of stratiform and convective rainfall by combining the rainfall classifications (stratiform and convective) of TRMM/PR, with its aim of obtaining land rainfall retrieval formulas under different types of rainfall.

References

Data Bank for Atmospheric Research, Web Browser: http://dbar.as.ntu.edu.tw/.

Central Weather Bureau, Web Browser: http://www.cwb.gov.tw/index-f.htm.

Chen Wann-Jin and C. C. Li, 2000 : Oceanic rain rate retrievals using TRMM Microwave Imager multi-channel brightness temperatures obtained during the 1998 SCSMEX, TAO, Vol. 11, No. 4, 765-788.

Chen Wann-Jin and C. C. Li, 2002: Rain retrievals using Tropical Rainfall Measuring Mission and Geostationary Meteorological Satellite 5 data obtained during the SCSMEX, International Journal of Remote Sensing, Vol. 23, No. 12, 2425-2448.

Ferraro, R. R., and G. F. Marks, 1995: The development of SSM/I rain-rate retrieval algorithms using ground-based radar measurements, J. Atmo. Ocean. Tech., 12(4), 755–770.

Grody, N. C., 1991: Classification of snow cover and precipitation using the Special Sensor Microwave Imager, J. Geophys. Res., Vol. 96, pp. 7423-7435.

Kummerow, C., Barnes, W., Kozu, T., Shiue, J., and Simpson, J., 1998: The tropical rainfall measuring mission (TRMM) sensor package, J. Atmo. Ocean. Tech., Vol. 15, pp. 809-817.

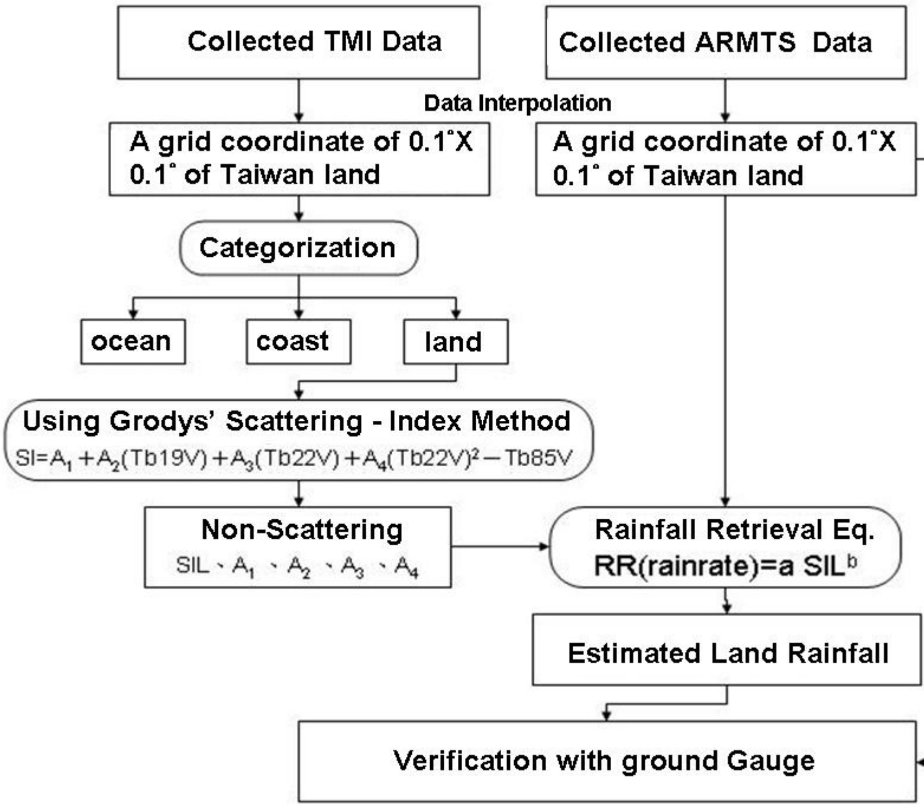

Fig.1 The flow chart is a schematic of rainfall retrieval over Taiwan land.

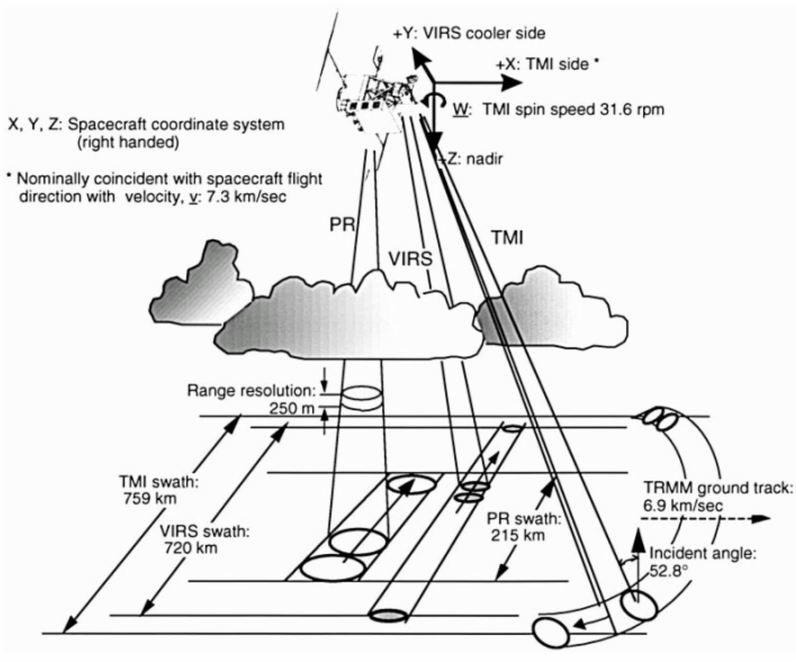

Fig. 2 The scan patterns and resolutions of TRMM sensors, including TMI, PR, and VIRS.

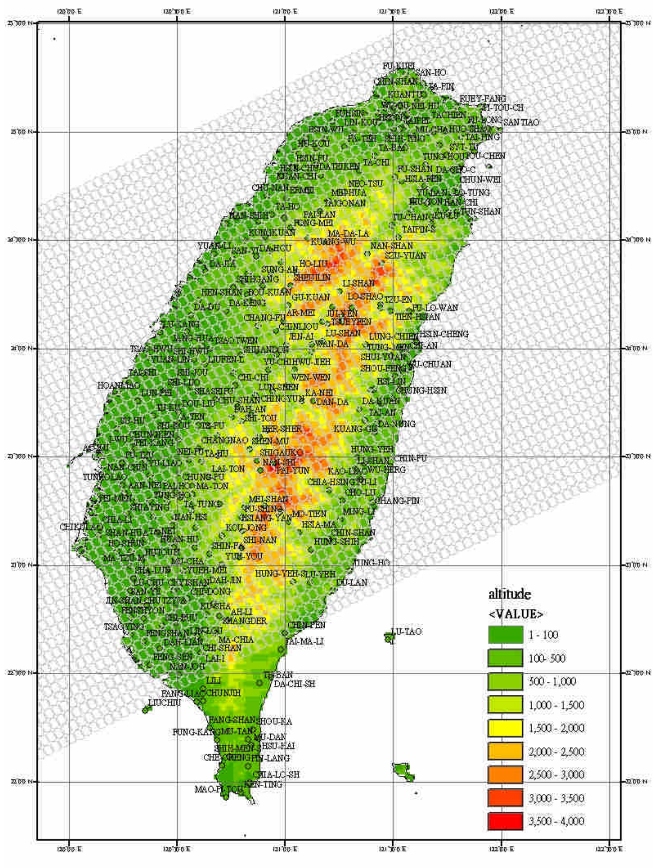

Fig. 3 The illustration is a scatter of ground rain gauge in Taiwan

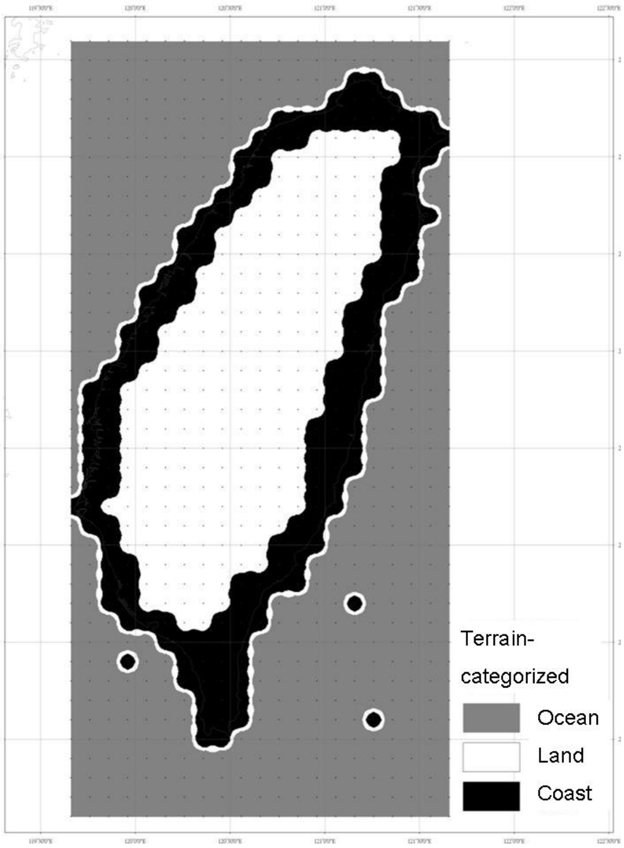

Fig. 4 There are 861 grid coordinates of 0.1° * 0.1°, to depend on the earth terrain are categorized into: 217 points over land (white), 157 points along coast (black) and 487 points over ocean (grey)

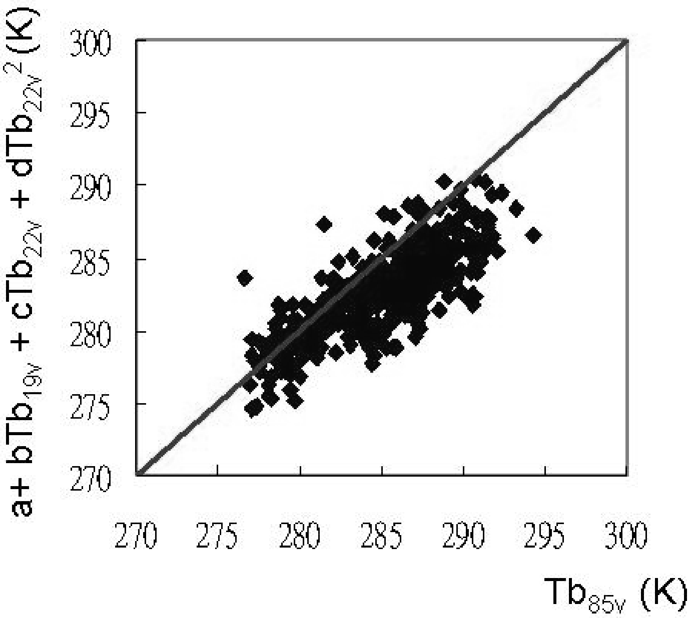

Fig.5 Non-Scattering Atmospheric Conditions, The scatter diagrams is Simulating Tb85V by Tb19V and Tb21V in TRMM/TMI microwave channels.

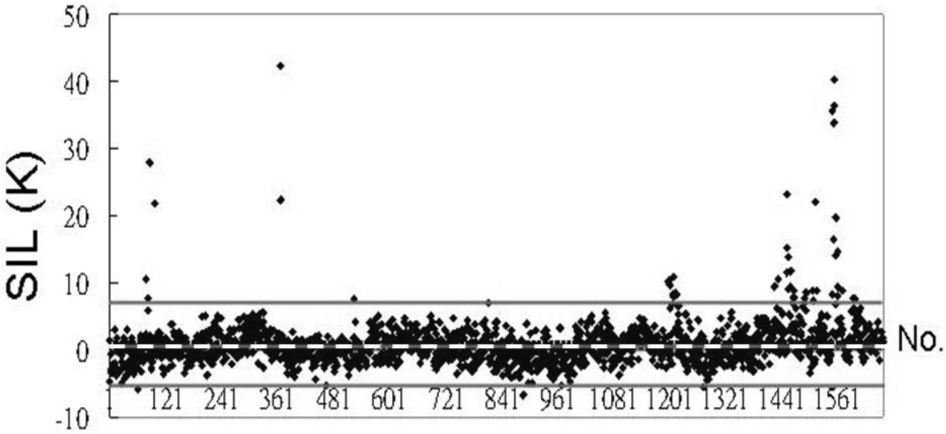

Fig.6 The scatter diagrams of the SIL Value, when rainfall is 0 mm/hr.

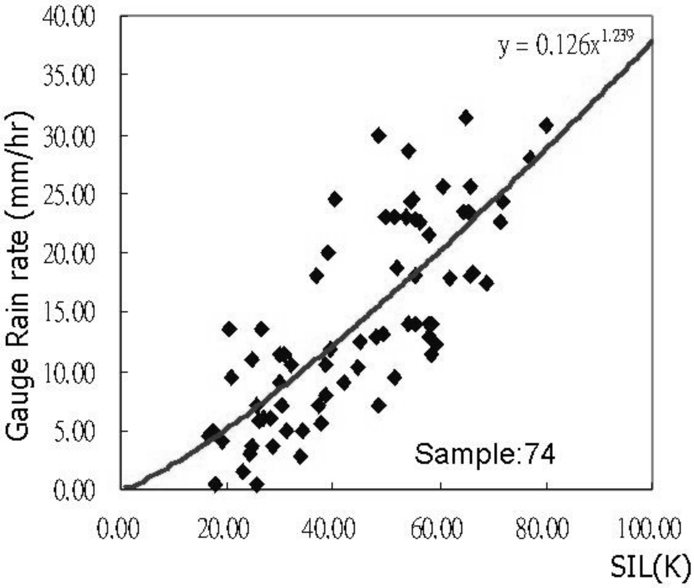

Fig.7 Depicts the relationship between SIL from TRMM/TMI satellite data and land rainfall observed from ARMTS.

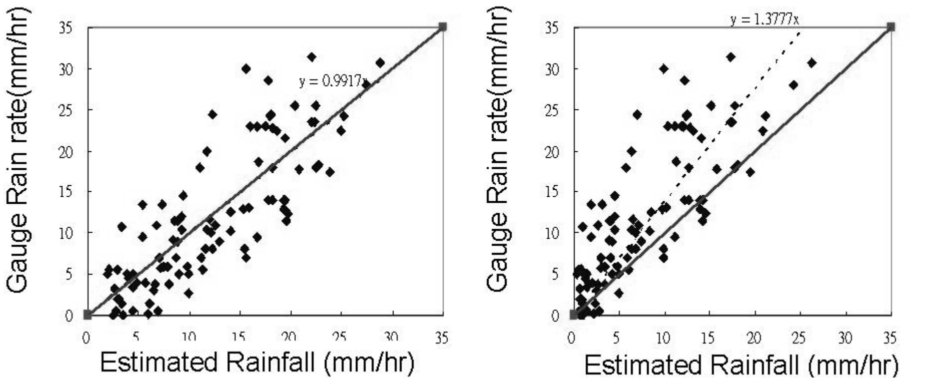

Fig. 8 compared satellite-estimated rainfall with ground truth (rain gauge). left: LRCT, right: LRFM. (The dash line is the regression lines, and the solid lines represent a 1:1 relationship).

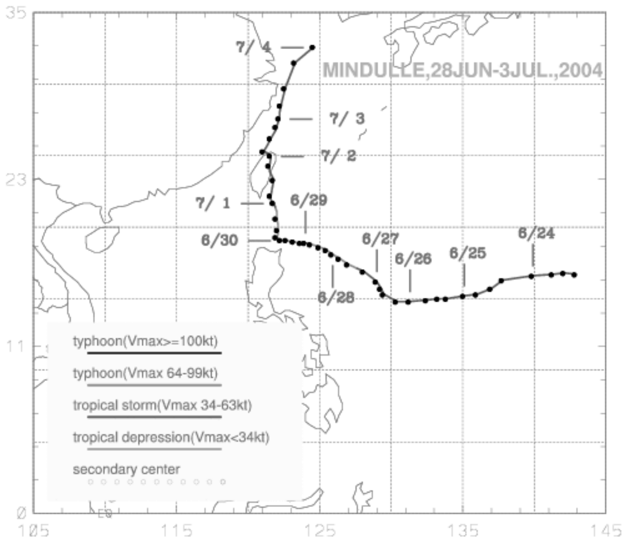

Fig. 9 The track chart of Typhoon Mindulle.

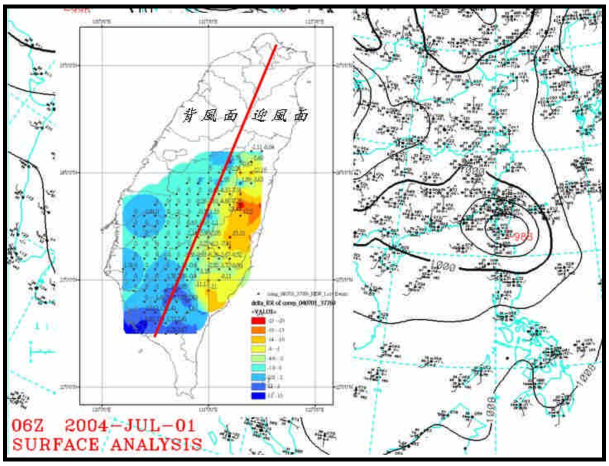

Fig. 10 The rainfall difference distribution map, 2004 / 07 / 01 04:52 UTC (#37769).

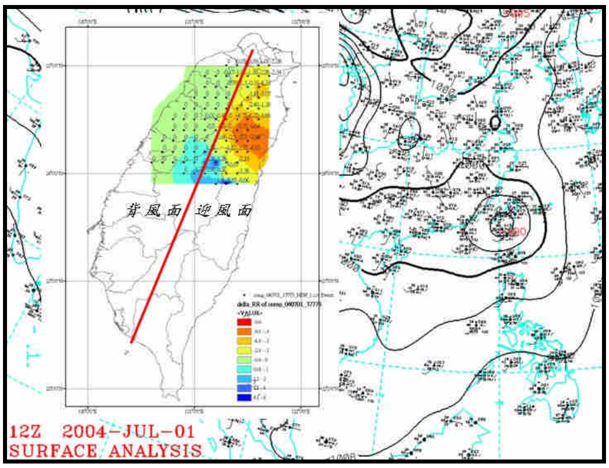

Fig. 11 The rainfall difference distribution map, 2004 / 07 / 01 11:24 UTC (#37773).

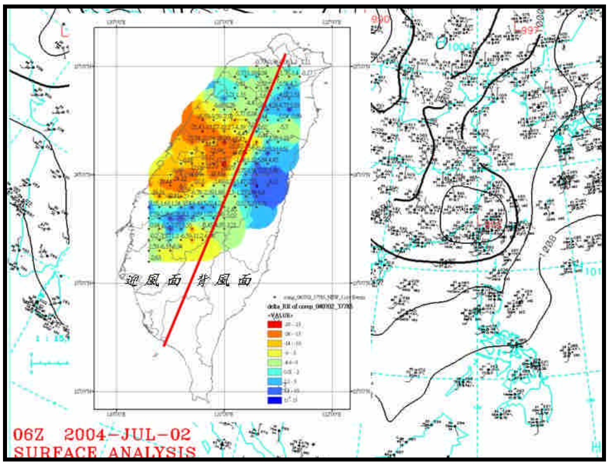

Fig. 12 The rainfall difference distribution map, 2004 / 07 / 02 05:35 UTC (#37785).

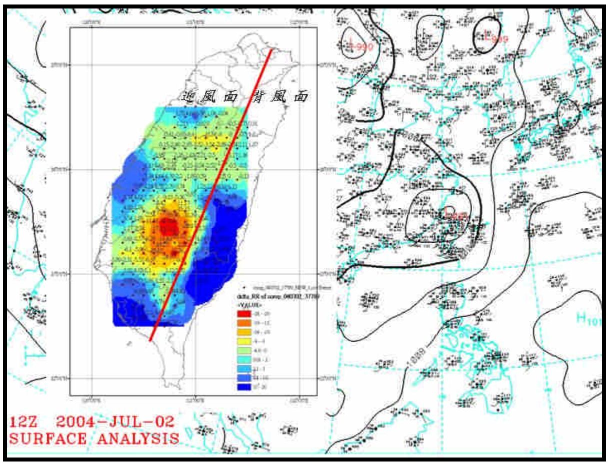

Fig. 13 The rainfall difference distribution map, 2004 / 07 / 02 12:07 UTC (#37789).

Table 1 Verification of land rainfall estimates during the Typhoon Mindulle

retrieval algorithm	mean rainfall rate (mm/hr)	RMS (mm/hr)
Ground Truth	14.15	—
LRCT	14.14	5.14
LRFM	9.33	7.13

Table 2 Verification of land rainfall estimates during the Typhoon Aere.

retrieval algorithm	mean rainfall rate (mm/hr)	RMS (mm/hr)
Ground Truth	5.53	__
LRCT	6.10	3.48
LRFM	2.71	4.28